Inorg. Chem. **2007**, *46*, 10479–10490

Mononuclear Rh(II) PNP-Type Complexes. Structure and Reactivity

Moran Feller,[†] Eyal Ben-Ari,[†] Tarkeshwar Gupta,[†] Linda J. W. Shimon,[‡] Gregory Leitus,[‡] Yael Diskin-Posner,[‡] Lev Weiner,[‡] and David Milstein*[,†]

Department of Organic Chemistry and Unit of Chemical Research Support, The Weizmann Institute of Science, Rehovot 76100, Israel

Received May 29, 2007

The Rh(II) mononuclear complexes [(PNP^{t}Bu)RhCl][BF_4] (**2**), [(PNP^{t}Bu)Rh(OC(O)CF_3)][OC(O)CF_3] (**4**), and [(PNP^{t}Bu)Rh(acetone)][BF_4]$_2$ (**6**) were synthesized by oxidation of the corresponding Rh(I) analogs with silver salts. On the other hand, treatment of (PNP^{t}Bu)RhCl with AgOC(O)CF_3 led only to chloride abstraction, with no oxidation. **2** and **6** were characterized by X-ray diffraction, EPR, cyclic voltammetry, and dipole moment measurements. **2** and **6** react with NO gas to give the diamagnetic complexes [(PNP^{t}Bu)Rh(NO)Cl][BF_4] (**7**) and [(PNP^{t}Bu)Rh(NO)(acetone)][BF_4]$_2$ (**8**) respectively. **6** is reduced to Rh(I) in the presence of phosphines, CO, or isonitriles to give the Rh(I) complexes [(PNP^{t}Bu)Rh(PR_3)][BF_4] (**11**, **12**) (R = Et, Ph), [(PNP^{t}Bu)Rh(CO)][BF_4] (**13**) and [(PNP^{t}Bu)Rh(L)][BF_4] (**15, 16**) (L = *tert*-butyl isonitrile or 2,6-dimethylphenyl isonitrile), respectively. On the other hand, **2** disproportionates to Rh(I) and Rh(III) complexes in the presence of acetonitrile, isonitriles, or CO. **2** is also reduced by triethylphosphine and water to Rh(I) complexes [(PNP^{t}Bu)RhCl] (**1**) and [(PNP^{t}Bu)Rh(PEt_3)][BF_4] (**11**). When triphenylphosphine and water are used, the reduced Rh(I) complex reacts with a proton, which is formed in the redox reaction, to give a Rh(III) complex with a coordinated BF_4, [(PNP^{t}Bu)Rh(Cl)(H)(BF_4)] (**9**).

Introduction

Whereas Rh(I) and Rh(III) complexes are ubiquitous and have found many uses, Rh(II) complexes are less common. In particular, mononuclear Rh(II) complexes are relatively rare.[1−5] Rh(II) monomers are mainly stabilized by sterically crowded ligands. The most common Rh(II) monomers are the porphyrin complexes, their stability being derived from the sterically demanding substituted ligand, the chelating effect, and the delocalized π system of the porphyrin. Rh(II) porphyrins exhibit diverse reactivity as metalloradicals toward H_2, CO, and hydrocarbons.[6] Recently de Bruin et al. reported a new family of Rh(II)(olefin)(N_3) complexes, which exhibit interesting reactivity in vinylic C−H activation and in the oxygenation of the norbornadiene ligand to norbornenone.[3] Bergman, Tilley, and coworkers reported the cyclopropanation of olefins with ethyl diazoacetate catalyzed

* To whom correspondence should be addressed. E-mail: david.milstein@weizmann.ac.il, Fax: 972-8-9344142.
† Department of Organic Chemistry.
‡ Unit of Chemical Research Support.

(1) For reviews on mononuclear rhodium (II) complexes see (a) de Bruin, B.; Hetterscheid, D. G. H. *Eur. J. Inorg. Chem.* **2007**, 211−230. (b) DeWit, D. G. *Coord. Chem. Rev.* **1996**, *147*, 209−246. (c) Pandey, K. K. *Coord. Chem. Rev.* **1992**, *121*, 1−42.

(2) For recent examples, see (a) Collman, J. P.; Boulatov, R. *J. Am. Chem. Soc.* **2000**, *122*, 11812−11821. (b) Connelly, N. G.; Emslie, D. J. H.; Geiger, W. E.; Hayward, O. D.; Linehan, E. B.; Orpen, A. G.; Quayle, M. J.; Rieger, P. H. *J. Chem. Soc., Dalton Trans.* **2001**, 670−683. (c) Willems, S. T. H.; Russcher, J. C.; Budzelaar, P. H. M.; de Bruin, B.; de Gelder, R.; Smits, J. M. M.; Gal, A. W. *Chem. Commun.* **2002**, 148−149. (d) Gerisch, M.; Krumper, J. R.; Bergman, R. G.; Tilley, T. D. *Organometallics* **2003**, *22*, 47−58. (e) Doux, M.; Mézailles, N.; Ricard, L.; Le Floch, P.; Adkine, P.; Berclaz, T.; Geoffroy, M. *Inorg. Chem.* **2005**, *44*, 1147−1152. (f) Hamazawa, R. T.; Nishioka, T.; Kinoshita, I.; Takui, T.; Santo, R.; Ichimura, A. *Dalton Trans.* **2006**, 1374−1376.

(3) (a) Hetterscheid, D. G. H.; Smits, J. M. M.; de Bruin, B. *Organometallics* **2004**, *23*, 4236−4246. (b) Hetterscheid, D. G. H.; de Bruin, B.; Smits, J. M. M.; Gal, A. W. *Organometallics* **2003**, *22*, 3022−3024. (c) Hetterscheid, D. G. H.; de Bruin, B. *J. Mol. Catal. A: Chem.* **2006**, *251*, 291−296. (d) Hetterscheid, D. G. H.; Klop, M.; Kicken, R. J. N. A. M.; Smits, J. M. M.; Reijerse, E. J.; de Bruin, B. *Chem.—Eur. J.* **2007**, *13*, 3386−3405.

(4) Krumper, J. R.; Gerisch, M.; Suh, J. M.; Bergman, R. G.; Tilley, T. D. *J. Org. Chem.* **2003**, *68*, 9705−9710.

(5) (a) Dixon, F. M.; Masar, M. S., III; Doan, P. E.; Farrell, J. R.; Arnold, F. P., Jr; Mirkin, C. A.; Incarvito, C. D.; Zakharov, L. N.; Rheingold, A. L. *Inorg. Chem.* **2003**, *42*, 3245−3255. (b) Dixon, F. M.; Farrell, J. R.; Doan, P. E.; Williamson, A.; Weinberger, D. A.; Mirkin, C. A.; Stern, C.; Incarvito, C. D.; Liable-Sands, L. M.; Zakharov, L. N.; Rheingold, A. L. *Organometallics* **2002**, *21*, 3091−3093. (c) Singewald, E. T.; Slone, C. S.; Stern, C. L.; Mirkin, C. A.; Yap, G. P. A.; Liable-Sands, L. M.; Rheingold, A. L. *J. Am. Chem. Soc.* **1997**, *119*, 3048−3056.

(6) For example, activation of various substrates by (TMP)Rh(II) (a) dihydrogen: Wayland, B. B.; Ba, S.; Sherry, A. E. *Inorg. Chem.* **1992**, *31*, 148−150. (b) methane: Wayland, B. B.; Ba, S.; Sherry, A. E. *J. Am. Chem. Soc.* **1991**, *113*, 5305−5311. (c) ethane and CO: Cui, W.; Li, S.; Wayland, B. B. *J. Organomet. Chem.* **2007**, *692*, 3198−3206.

10.1021/ic701044b CCC: $37.00
Published on Web 09/29/2007

by a stable monomeric bisoxazoline Rh(II) complex.[4] Another example of stable Rh(II) monomers includes bis-phosphinoalkylarene complexes with a two-legged piano-stool geometry, which are stabilized by electron-rich and sterically demanding arenes along with flexible tether arms.[5]

Late transition-metal complexes of electron donating and bulky pincer ligands have found important applications in synthesis, bond activation, and catalysis.[7] Among these, complexes of the ligand PNP^{t}Bu (PNP^{t}Bu = 2,6-bis-(di-*tert*-butyl phosphino methyl)pyridine)[8] have recently shown diverse reactivity. For example, the complex [(PNP^{t}Bu)Ir-(COE)][BF_4] (COE = cyclooctene) selectively activates the *ortho* C−H bonds of haloarenes[9] and the sp^3 C−H bonds of ketones at the β position.[10] It also demonstrates unusual C−H and H_2 activation via ligand−metal cooperativity, involving dearomatization/aromatization of the ligand.[11] PNP^{t}Bu ruthenium complexes exhibit high catalytic activity in the acceptorless dehydrogenation of secondary alcohols to ketones[12] and primary alcohols to esters.[13] Ruthenium PNN complexes (PNN = 2-di-*tert*-butylphosphinomethyl-6-diethylaminomethyl-pyridine) are particularly efficient in the latter reaction under neutral conditions[13] and are also exceptionally active in catalytic hydrogenation of esters to alcohols under mild pressure and neutral conditions.[14] PNP^{t}Bu−Ru dihydrogen complexes[15] catalyze the H/D exchange of aromatic C−H bonds with D_2O or C_6D_6 under mild conditions.[16] A palladium ^{t}Bu−PNP system effectively catalyzed the addition of amines to acrylic acid derivatives,[17] and aryl C−H activation by ^{t}Bu−PNP rhodium complexes were reported.[18]

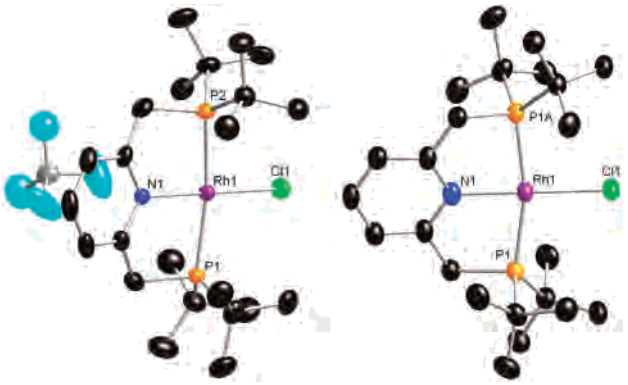

Figure 1. Molecular drawing of **2** (left) and **1** (right) at 50% probability level. Hydrogen atoms were omitted for clarity.

Scheme 1

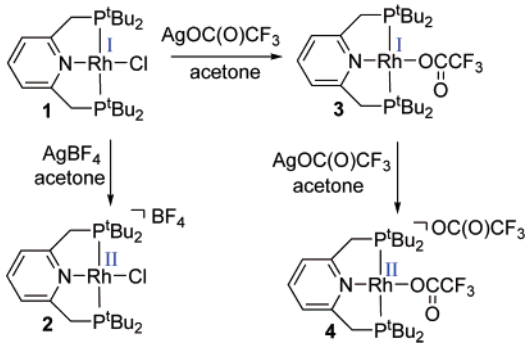

Herein, we report on the synthesis of (PNP^{t}Bu)Rh(II) complexes and their characterization by X-ray diffraction, EPR, cyclic voltammetry, and dipole moment measurements. Their reactivity toward CO, acetonitrile, isonitriles, and triphenylphosphine, including some unexpected observations, is reported.

Results and Discussion

1. Synthesis and Characterization of (PNP^{t}Bu)Rh(II) Complexes. We have recently reported the electron-rich, neutral Rh(I) complex of 2,6-bis-(di-*tert*-butyl phosphino methyl)pyridine, (PNP^{t}Bu)RhCl (**1**).[8] Somewhat surprisingly, the reaction of **1** with $AgBF_4$ in acetone furnished a mononuclear paramagnetic complex [(PNP^{t}Bu)RhCl][BF_4] (**2**) (Scheme 1) with no chloride abstraction being observed. The ^{1}H NMR spectrum of **2** exhibits only a solvent signal, and no signals are observed in the ^{31}P{^{1}H} NMR spectrum. The identity of **2** was confirmed by a single-crystal X-ray analysis (Figure 1). The rhodium atom adopts a square-planar geometry, which is consistent with reported four-coordinated mononuclear Rh(II) X-ray structures.[2d,19] The P−Rh−P angle (168.33°) is distorted from linearity, as is typical for PNP complexes.[8−11] Selective bond lengths and bond angles are given in Table 1. Neutral Rh(I) complex **1** was crystallized,

(7) Reviews, (a) Pugh, D.; Danopoulos, A. A. *Coord. Chem. Rev.* **2007**, *251*, 610−641. (b) Szabó, K. J. *Synlett* **2006**, *6*, 811−824. (c) Rybtchinski, B.; Milstein, D. *ACS Symp. Ser.* **2004**, *885*, 70−85. (d) van der Boom, M. E.; Milstein, D. *Chem. Rev.* **2003**, *103*, 1759−1792. (e) Singleton, J. T. *Tetrahedron* **2003**, *59*, 1837−1857. (f) Milstein, D. *Pure Appl. Chem.* **2003**, *75*, 445−460. (g) Albrecht, M.; van Koten, G. *Angew. Chem., Int. Ed.* **2001**, *40*, 3750−3781. (h) Vigalok, A.; Milstein, D. *Acc. Chem. Res.* **2001**, *34*, 798−807. (i) Jensen, C. M. *Chem. Commun.* **1999**, 2443−2449. (j) Rybtchinski, B.; Milstein, D. *Angew. Chem., Int. Ed.* **1999**, *38*, 871−883.
(8) Hermann, D.; Gandelman, M.; Rozenberg, H.; Shimon, L. J. W.; Milstein, D. *Organometallics* **2002**, *21*, 812−818.
(9) (a) Ben-Ari, E.; Gandelman, M.; Rozenberg, H.; Shimon, L. J. W.; Milstein, D. *J. Am. Chem. Soc.* **2003**, *125*, 4714−4715. (b) Ben-Ari, E.; Gandelman, M.; Shimon, L. J. W.; Martin, J. M. L.; Milstein, D. *Organometallics* **2006**, *25*, 3190−3210.
(10) Feller, M.; Karton, A.; Leitus, G.; Martin, J. M. L.; Milstein, D. *J. Am. Chem. Soc.* **2006**, *128*, 12400−12401.
(11) Ben-Ari, E.; Leitus, G.; Shimon, L. J. W.; Milstein, D. *J. Am. Chem. Soc.* **2006**, *128*, 15390−153901.
(12) Zhang, J.; Gandelman, M.; Shimon, L. J. W.; Rozenberg, H.; Milstein, D. *Organometallics* **2004**, *23*, 4026−4033.
(13) Zhang, J.; Leitus, G.; Ben-David, Y.; Milstein, D. *J. Am. Chem. Soc.* **2005**, *127*, 10840−10841.
(14) Zhang, J.; Leitus, G.; Ben-David, Y.; Milstein, D. *Angew. Chem., Int. Ed.* **2006**, *45*, 1113−1115.
(15) Prechtl, M. H. G.; Ben-David, Y.; Giunta, D.; Busch, S.; Taniguchi, Y.; Wisniewski, W.; Gorls, H.; Mynott, R. J.; Theyssen, N.; Milstein, D.; Leitner, W. *Chem.−Eur. J.* **2007**, *13*, 1539−1546.
(16) Prechtl, M. H. G.; Hölscher, M.; Ben-David, Y.; Theyssen, N.; Loschen, R.; Milstein, D.; Leitner, W. *Angew. Chem., Intl. Ed.* **2007**, *46*, 2269−2272.
(17) (a) Kawatsura, M.; Hartwig, J. F. *Organometallics* **2001**, *20*, 1960−1964. (b) Stambuli, J. P.; Stauffer, S. R.; Shaughnessy, K. H.; Hartwig, J. F. *J. Am. Chem. Soc.* **2001**, *123*, 2677−2678.
(18) Kloek, S. M.; Heinekey, D. M.; Goldberg, K. I. *Angew. Chem., Int. Ed.* **2007**, *46*, 4736−4738.
(19) (a) García, M. P.; Jiménez, M. V.; Cuesta, A.; Siurana, C.; Oro, L. A.; Lahoz. F. J.; López, J. A.; Catalán, M. P. *Organometallics* **1997**, *16*, 1026−1036. (b) García, M. P.; Jiménez, M. V.; Oro, L. A.; Lahoz, F. J.; Casas, J. M.; Alonso, P. J. *Organometallics* **1993**, *12*, 3257−3263. (c) Hay-Motherwell, R. S.; Koschmieder, S. U.; Wilkinson, G.; Hussain-Bates, B.; Hursthouse, M. B. *J. Chem. Soc., Dalton Trans.* **1991**, 2821−2830. (d) Ogle, C. A.; Masterman, T. C.; Hubbard, J. L. *J. Chem. Soc., Chem. Commun.* **1990**, 1733−1734.

Table 1. Selected Bond Lengths (Angstroms) and Bond Angles (Degrees) for [(PNP^{t}Bu)RhCl] (**1**) and [(PNP^{t}Bu)RhCl][BF_4] (**2**)

	[(PNP^{t}Bu)RhCl] (**1**)	[(PNP^{t}Bu)RhCl][BF_4] (**2**)
Rh(1)−P(1)	2.271(1)	2.322(1)
Rh(1)−P(2)[a]	2.271(1)	2.322(1)
Rh(1)−Cl(1)	2.381(1)	2.332(1)
Rh(1)−N(1)	2.036(3)	2.074(3)
P(1)−Rh(1)−Cl(1)	96.71(2)	95.74(4)
P(2)−Rh(1)−Cl(1)[a]	96. 71(2)[b]	95.33(4)
N(1)−Rh(1)−Cl(1)	180.00(1)	178.65(8)
N(1)−Rh(1)−P(2)[a]	83.29(2)[b]	84.58(8)
N(1)−Rh(1)−P(1)	83.29(2)	84.26(8)
P(1)−Rh(1)−P(2)[a]	166.57(4)[b]	168.32(4)

[a] P(2) in **1** is marked as P1A in Figure 1. [b] Symmetry transformations used to generate equivalent atoms.

Scheme 2

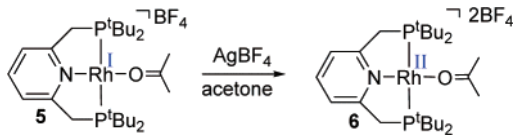

and its X-ray structure was determined also, providing an opportunity to compare the two complexes, which have the same atom connectivity and differ only in the metal oxidation state. The structure of **1** (Figure 1, Table 1) reveals that the Rh−N, Rh−P(1), and Rh−P(2) bonds of the PNP ligand are shorter compared to the corresponding bonds of **2** (by 0.036 and 0.051 Å, respectively). Similar elongation due to oxidation was described for Rh(I) and Rh(II) piano stool complexes with bis(phosphinoalkyl)aryl ligands,[5a] complexes $(PEt_3)_2(C_5H_5)Co(I)$ and $[(PEt_3)_2(C_5H_5)Co(II)][BF_4]$,[20] and complexes $(^iPr_3P)_2RhCl_2$ and $(^iPr_3P)_2RhCl_2H$.[21] However, the Rh−Cl bond in **2** is shorter by 0.049 Å compared with **1**. The shortening of the Rh−Cl bond due to oxidation can be explained by enhanced π donation of the chloride ligand in **2**.[22] The N−Rh−Cl angle in **1** is strictly linear and it is almost linear in **2**, whereas the P(1)−Rh−P(2) angle is distorted from linearity to a similar degree in both complexes. In **2**, the phosphines P(1) and P(2) are above the pyridine ring, whereas **1** adopts a propeller-type geometry with P(1A) and P(1) above and below the pyridine plane, respectively.

1 was also oxidized by $AgPF_6$ and $AgBAr^f$ (BAr^f = tetrakis{(3,5-trifluoromethyl)phenyl}borate)) in acetone to give the paramagnetic **2**. On the other hand, treatment of **1** with $AgOC(O)CF_3$ in acetone resulted in chloride abstraction rather than oxidation, exclusively yielding the diamagnetic complex [(PNP^{t}Bu)Rh(OC(O)CF_3)] (**3**) (Scheme 1). In the $^{31}P\{^1H\}$ NMR spectrum, **3** exhibits a sharp doublet at 61.27 ppm with a J_{RhP} of 151.1 Hz in THF and a broad signal at

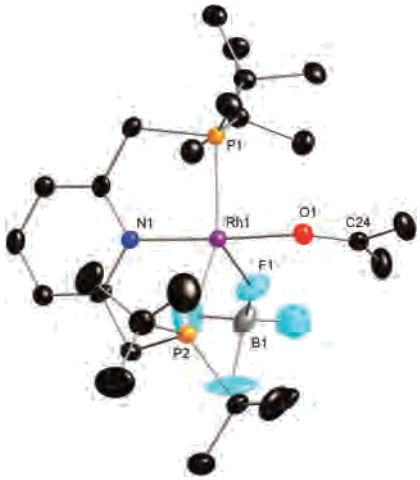

Figure 2. Molecular drawing of **6** at 50% probability level. Hydrogen atoms and the non-coordinating anion were omitted for clarity.

Table 2. Selected Bond Lengths (Angstroms) and Bond Angles (Degrees) for [(PNP^{t}Bu)Rh(acetone)][BF_4]$_2$ (**6**)

Rh(1)−P(2)	2.351(1)	Rh(1)−O(1)	2.088(2)
O(1)−C(24)	1.235(4)	Rh(1)−N(1)	2.047(2)
Rh(1)−F(1)	2.523(9)	Rh(1)−P(1)	2.363(3)
F(1)−B(1)	1.422(4)		
P(1)−Rh(1)−P(2)	161.78(3)	N(1)−Rh(1)−P(2)	81.88(7)
N(1)−Rh(1)−O(1)	173.71(9)	O(1)−Rh(1)−P(1)	96.62(6)
Rh(1)−O(1)−C(24)	139.6(2)	O(1)−Rh(1)−P(2)	97.51(6)
N(1)−Rh(1)−P(1)	82.81(7)		

61 ppm in acetone due to fluxional coordination of the trifluoroacetate in acetone. **3** was oxidized easily to the paramagnetic complex [(PNP^{t}Bu)Rh(OC(O)CF_3)][OC(O)-CF_3] (**4**) by the addition of an additional equiv of AgOC-(O)CF_3 (Scheme 1). Similarly, reaction of **3** with other AgX (X = BF_4, PF_6, BAr^f) led to [(PNP^{t}Bu)Rh(OC(O)CF_3)][X].

Cationic Rh(I) complex [(PNP^{t}Bu)Rh(acetone)][BF_4] (**5**) was prepared in order to oxidize it to Rh(II). It was obtained in quantitative yield by the addition of the free ligand PNP^t-Bu to an acetone solution of $[Rh(COE)_2(acetone)_2][BF_4]$.[23] The acetone molecule in **5** is loosely bound and can be replaced with other solvents such as THF or with N_2 by bubbling nitrogen through a THF solution of **5**.[18] **5** is oxidized easily by $AgBF_4$ to the paramagnetic Rh(II) complex [(PNP^{t}Bu)Rh(acetone)][BF_4]$_2$ (**6**) (Scheme 2). The X-ray structure of **6** (Figure 2, Table 2) exhibits a Rh(II) center in a square-pyramidal geometry with a loosely bound BF_4 at the apical position. Coordination of BF_4 is rare,[24] and to the best of our knowledge, only two other crystal structures containing a Rh−FBF_3 bond were reported.[24a,b] The Rh−F(1) bond in **6** (2.523 Å) is significantly longer than the reported Rh−F bonds in other coordinated BF_4 complexes[24a,b] by about 0.37 Å, which indicates the very weak nature of

(20) Harlow, R. L.; McKinney, R. J.; Whitney, J. F. *Organometallics* **1983**, *2*, 1839−1842.
(21) Harlow, R. L.; Thorn, D. L.; Baker, R. T.; Jones, N. L. *Inorg. Chem.* **1992**, *31*, 993−997.
(22) For examples of stabilization by π donation of chloride see (a) Riehl, J. F.; Jean, Y.; Eisenstein, O.; Pélissier, M. *Organometallics* **1992**, *11*, 729−737. (b) Blum, O.; Milstein, D. *J. Am. Chem. Soc.* **2002**, *124*, 11456−11467. (c) Bickford, C. C.; Johnson, T. J.; Davidson, E. R.; Caulton, K. G. *Inorg. Chem.* **1994**, *33*, 1080−1086. (d) Bera, J. K.; Nethaji, M.; Samuelson, A. G. *Inorg. Chem.* **1999**, *38*, 218−228. (e) Werner, H.; Höhn, A.; Dziallas, M. *Angew. Chem., Int. Ed. Engl.* **1986**, *12*, 1090.
(23) Windmüller, B.; Nürnberg, O.; Wolf, J.; Werner, H. *Eur. J. Inorg. Chem.* **1999**, 613−619.
(24) (a) Salem, H.; Ben-David, Y.; Shimon, L. J. W.; Milstein, D. *Organometallics* **2006**, *25*, 2292−2300. (b) Rybtchinski, B.; Oevers, S.; Montag, M.; Vigalok, A.; Rozenberg, H.; Martin, J. M. L.; Milstein, D. *J. Am. Chem. Soc.* **2001**, *123*, 9064−9077. (c) Gandelman, M.; Konstantinovski, L.; Rozenberg, H.; Milstein, D. *Chem.−Eur. J.* **2003**, *9*, 2595−2602. (d) Beck, W.; Sunkel, K. *Chem. Rev.* **1988**, *88*, 1405−1421. (e) Sutherland, B. R.; Cowie, M. *Inorg. Chem.* **1984**, *23*, 1290−1297.

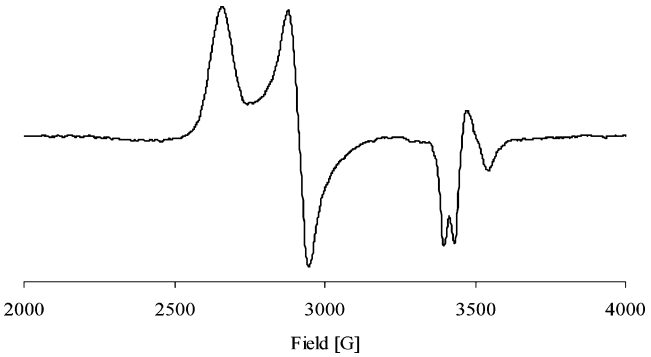

Figure 3. X-band EPR spectrum of **2** obtained at 125 K in frozen acetone. Experimental conditions: microwave power 31 mW, modulation amplitude 0.8 G, time constant 0.65 s.

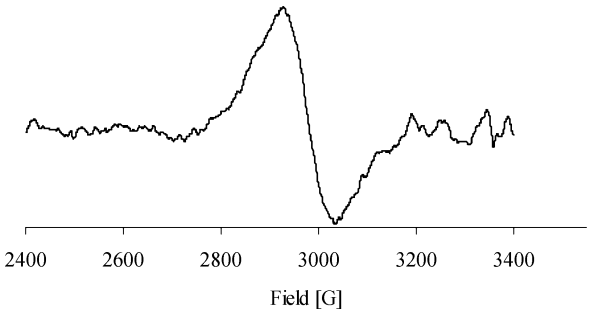

Figure 4. X-band EPR spectrum of **4** obtained at 293 K in acetone. Experimental conditions: microwave power 39 mW, modulation amplitude 1 G, time constant 1.3 s.

Table 3. EPR Parameters of **2**, **4**, and **6**

Complex	g_x	g_y	g_z	A_1G
2	2.5667	2.3124	1.9512	16.0
4	2.4851	2.3052	1.9654	17.0
6	2.5204	2.3231	1.9620	16.5

this bond. Because of BF_4 disorder, it is impossible to compare the F(1)−B bond length with the three other B−F bond lengths, which should be shorter in the case of Rh−F coordination. Although the Rh−F(1) bond is rather long, it is shorter than the sum of the ionic radius in the crystal structure of fluorine anion (1.33 Å)[25] and the pseudopotential radius of rhodium (2.52 Å).[26]

The distortion from planarity in **6** is much more extensive compared to **2**, with a P−Rh−P angle of 161.78° (168.32° in **2**) and a N−Rh−O angle of 173.67° (178.65° in **2** for N−Rh−Cl). The phosphines are alternating above and below the pyridine ring as in **1**. The bond angle Rh−O−C(24) is 139.6°, which indicates that the acetone ligand is coordinated through one of the lone pairs of electrons of the oxygen atom.

Oxidation of (PNP^{i}Pr)RhCl and [(PNP^{i}Pr)Rh(COE)][BF_4][27] gave mixtures of diamagnetic complexes according to $^{31}P\{^1H\}$ NMR. It is likely that the mononuclear [(PNP^{t}Bu)Rh(II) complexes are much more stable than (PNP^{i}Pr)Rh(II) because of steric shielding of the metal center.

The paramagnetic d^7 Rh(II) complexes **2**, **4** and **6** were studied by X-band EPR spectroscopy in both fluid and frozen acetone. For all three complexes in the frozen solution, an EPR rhombic pattern was observed, and no hyperfine structure was resolved for central- and low-field components g_x and g_y (Figure 3). For the g_z component, the observed doublet hyperfine splitting can be explained by coupling with the nuclear spin of ^{103}Rh ($I = {}^1/_2$). The observed EPR parameters of **2**, **4** and **6** (Table 3) were found to be close to the reported EPR parameters of other Rh(II) monomeric complexes.[2d,5a] The EPR data implies an asymmetric coordination environment around the metal center, which is in correlation with the distorted square-planar X-ray structures of **2** and **6**. The EPR isotropic spectrum of **4** in solution at ambient temperature is shown in Figure 4. The large line width is likely caused by the slow reorientation of the bulky complex and by unresolved coupling with the nuclear spin of rhodium.

Electrochemical measurements of **1**, **2**, **5** and **6** were carried out in acetone using ^{t}Bu$_4$NPF$_6$ as a supporting electrolyte. All of the measurements were performed using Ag/AgCl as a reference electrode. The electrochemical data for all of the complexes is given in Table 4. The cyclic voltammetric data indicates that the oxidation and reduction peaks of **1** are localized at values almost identical to those observed for the redox waves of **2** and is the same for **5** and **6**. This observation is similar to those found for related rhodium compounds with the metal in different oxidation states.[19b,28] **1**, **2**, **5** and **6** exhibit two redox processes in positive potential, as illustrated in Figure 5. Analysis of the first redox wave at scan rates of 100−900 mV s^{-1} gives clear evidence that it involves a Rh(I)/Rh(II) couple. Each couple is diffusion controlled, as evidenced by the constant current function (i_p vs $\nu^{-1/2}$) over scan rates of 100−900 mV s^{-1} (Supporting Information, Figure 1). The ΔE value for the first redox process is in the range expected for fast one-electron couples (Table 4). The i_c/i_a ration was found to be unity for the first redox waves of **1**, **2** and **5**, **6** and second redox waves of **5** and **6**, indicating that this process is reversible. The second redox wave of **5** and **6** can be assigned to the Rh(II) to Rh(III) couple, whereas the second redox waves of **1** and **2** show an irreversible process.

The presence of chloride in **1** and **2** may stabilize the Rh(III) state, resulting in an irreversible oxidation potential, in contrast to **5** and **6**. All of the complexes show an additional irreversible reduction potential at ∼ −1.13 V, which can be assigned to Rh(I)/Rh(0) reduction waves (Table 4).

Field dependences of magnetic moments (Figure 6) of **2** and **6**, measured between $T = 5$ and 300 K, were strictly linear in the interval of $-1\ T < H < 1\ T$. The complexes do not show any hysteresis phenomena. **6** exhibits clear Curie−Weis behavior at the temperature interval of 2 K < T < 300

(25) *Handbook of Chemistry and Physics*, 85th ed.; Lide, D. R., Ed.; CRC Press: Boca Raton, FL, 2004−2005; pp 12−14.

(26) Pseudopotential radii are calculated radii derived from first principles, which can be used for predicting structure and compound formation. *International Tables For Crystallography*, Kluwer Academic Publishers: Norwell, MA, 1992; Vol. C, p 682.

(27) The complex [(PNP^{i}Pr)RhCl] was synthesized in a similar procedure as **1**. [(PNP^{i}Pr)Rh(COE)][BF_4] was synthesized from [Rh(COE)$_2$(acetone)$_2$][BF_4] and the free ligand in a similar procedure as [(PNP)Ir(COE)][BF_4] (ref 9).

(28) (a) Haefner, S. C.; Dunbar, K. R.; Bender, C. *J. Am. Chem. Soc.* **1991**, *113*, 9540−9553. (b) Cooper, S. R.; Rawle, S. C.; Yagbasan, R.; Watkin, D. J. *J. Am. Chem. Soc.* **1991**, *113*, 1600−1604.

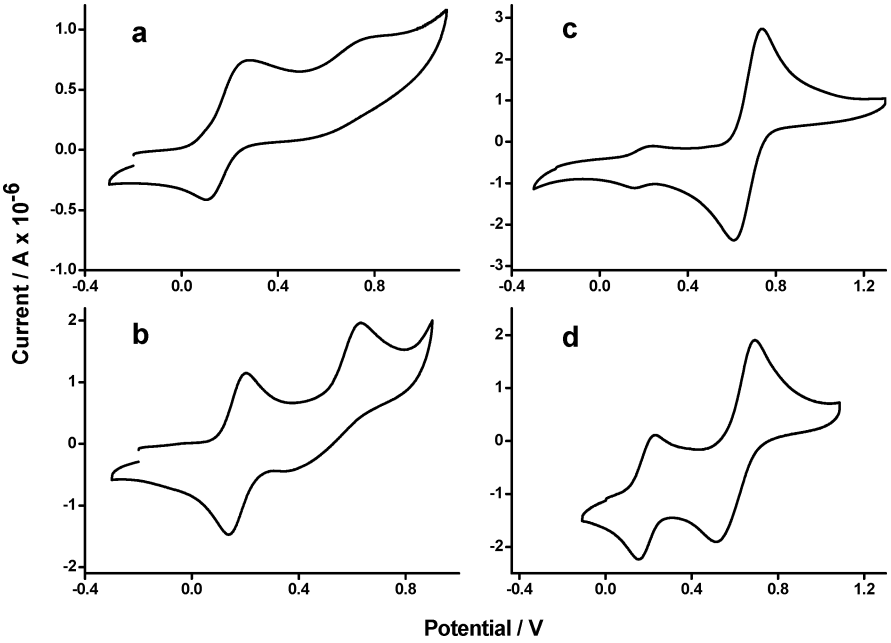

Figure 5. Cyclic voltammograms of **1** (a), **2** (b), **5** (c) and **6** (d) in acetone/0.1 M ^{t}Bu$_4$NPF$_6$ at room temperature (v = 0.3 Vs^{-1}; vs Ag/AgCl electrode).

Table 4. Formal Electrode Potentials[a] (vs Ag/AgCl) of the Complexes

complex	$E_{1/2}$ (ΔE); volts Rh(I)/Rh(II)	$E_{1/2}$ (ΔE); volts Rh(II)/Rh(III)	reduction waves[b] Rh(I)/Rh(0)
1	0.19 (0.13)	0.77[b]	−1.12
2	0.17 (0.069)	0.74[b]	−1.11
5	0.19 (0.081)	0.67 (0.12)	−1.12
6	0.17 (0.068)	0.65 (0.16)	−1.16

[a] Acetone solution containing the complex (2 mM) and ^{t}Bu$_4$NPF$_6$ (0.1 M); room temperature; ν = 0.3 Vs^{-1}. [b] Irreversible peak.

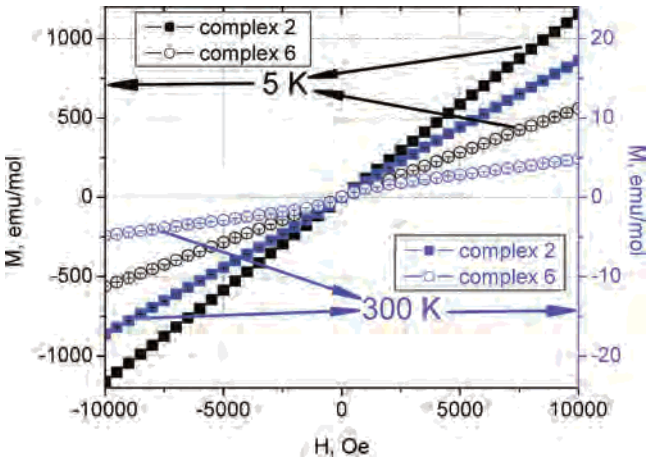

Figure 6. Field dependences of dc magnetic moments M at T = 5 and 300 K for **2** and **6**. Each graph displays results of measurements with increasing and decreasing field (from −1 T to +1 T and backward).

K (Figure 7). Lack of coincidence is observed at T < 10 K for **2**. The fitting of dc temperature dependences by the Curie−Weiss equation showed the values of effective magnetic moment for **6**, p = 1.72(2) μ_B/molecule and for **2** (using T > 10 K), p = 2.17(1) μ_B/molecule. Bergman, Tilley, and co-workers report values in the range of 1.87 to 2.00 μ_B for NCN bis(oxazoline) Rh(II) complexes.[2d] Our results for **2** and **6** show a broader interval of p values, which can be explained by the presence of super-exchange interactions via different anions. The in-phase ac susceptibility χ' shown in

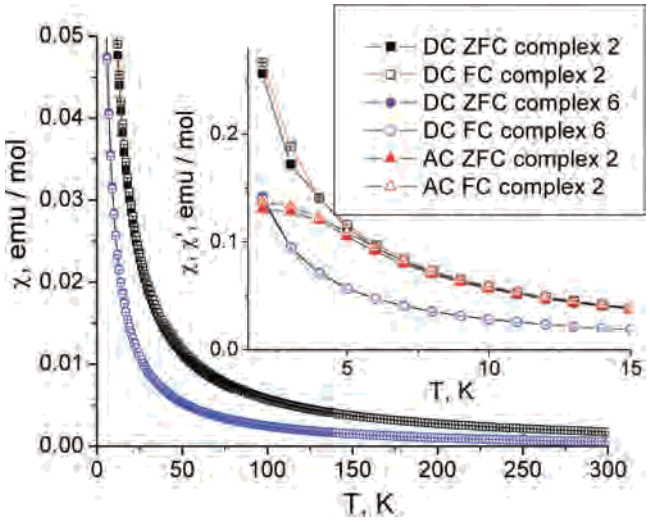

Figure 7. Zero field cooled and field cooled temperature dependences of dc magnetic susceptibilities χ obtained at H = 0.5 T for **2** and **6**. Inlay: The low-temperature part of the same dependences together with ac in-phase magnetic susceptibilities χ' for **2**, obtained at the H = 0.5 T, wave frequency f = 700 Hz, drive field amplitude H_A = 0.0003 T.

Figure 7 is clearly indicative of super-exchange interactions at low temperatures in **2**.

2. Reactivity of (PNP^{t}Bu)Rh(II) Complexes. Paramagnetic (PNP^{t}Bu)Rh(II) complexes **2**, **4** and **6** are stable and can be kept at ambient temperature as solids or in solution for months under nitrogen. No reaction was observed when these complexes were treated with oxygen, hydrogen, or ethylene. On the other hand, they exhibit rather unexpected reactivity toward CO, acetonitrile, isonitriles and phosphines.

Reactions of paramagnetic **2** and **6** with an excess of NO gas in acetone led to the formation of diamagnetic complexes [(PNP^{t}Bu)Rh(NO)Cl][BF$_4$] (**7**) and [(PNP^{t}Bu)Rh(NO)(acetone)][BF$_4$]$_2$ (**8**), respectively (Schemes 4, 5). **7** was obtained also by the addition of NOBF$_4$ to a solution of **1** in acetone. IR bands at 1675 and 1706 cm^{-1} for **7** and **8**, respectively,

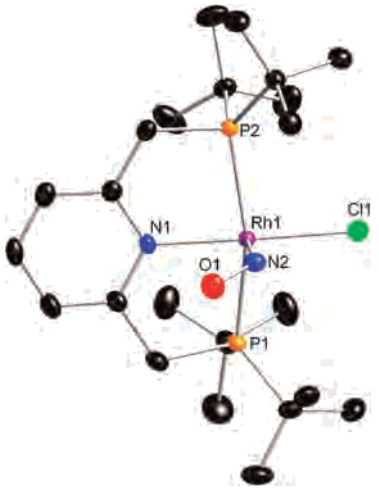

Figure 8. Molecular drawing of **7** at 50% probability level. Hydrogen atoms and counteranion were omitted for clarity.

Table 5. Selected Bond Lengths (Angstroms) and Bond Angles (Degrees) for [(PNP^{t}Bu)Rh(NO)Cl][BF_4](**7**)

Rh(1)−N(1)	2.068(2)	Rh(1)−P(2)	2.351(1)
Rh(1)−N(2)	1.943(3)	Rh(1)−Cl(1)	2.337(1)
Rh(1)−P(1)	2.339(1)	N(2)−O(1)	1.163(3)
P(1)−Rh(1)−P(2)	158.88(3)	N(1)−Rh(1)−P(2)	83.73(7)
P(1)−Rh(1)−N(2)	97.77(8)	P(2)−Rh(1)−N(2)	99.23(8)
P(1)−Rh(1)−Cl(1)	95.60(3)	P(2)−Rh(1)−Cl(1)	95.48(3)
N(1)−Rh(1)−N(2)	89.62(10)	Rh(1)−N(2)−O(1)	122.0(2)
N(1)−Rh(1)−Cl(1)	175.92(7)	N(2)−Rh(1)−Cl(1)	94.46(8)
N(1)−Rh(1)−P(1)	83.94(7)		

Scheme 3

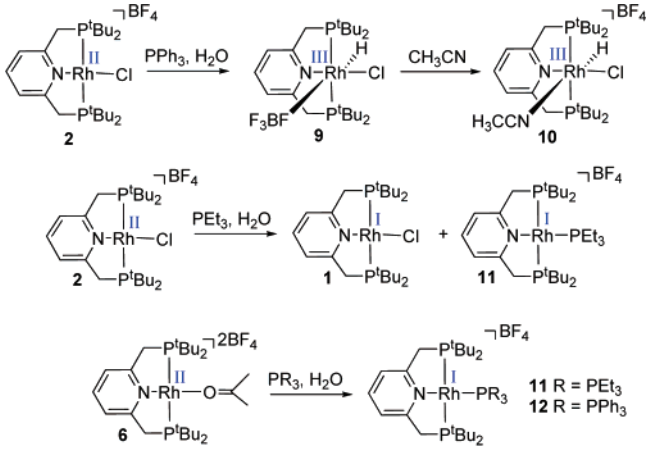

indicate that they are best described as Rh(III) complexes with a bent NO. A single-crystal X-ray analysis of **7** (Figure 8, Table 5) confirmed that it is a Rh(III) complex with a square-pyramidal geometry and a bent nitrosyl ligand, the O−N(2)−Rh angle being 122.0°. The chloride ligand is located trans to the ipso nitrogen, whereas the NO is at an apical position, which is typical for a bent NO ligand because of its strong trans influence. Similar rhodium and iridium nitrosyl complexes were reported.[29] The P−Rh−P angle (158.93°) is distorted from linearity, and the N(1)−Rh−Cl angle is almost linear (175.96°).

Surprisingly, the addition of a half equiv of triphenyphosphine to a solution of Rh(II)Cl **2** in acetone yielded diamagnetic Rh(III) hydride complex [(PNP^{t}Bu)Rh(Cl)(H)-(BF_4)] (**9**) (Scheme 3). The $^{31}P\{^1H\}$ NMR spectrum of this complex exhibits a sharp doublet at 67.8 ppm (J_{PRh} = 99.9 Hz), in addition to singlet signals at 26 ppm, which correspond to triphenylphosphine oxide. **9** was crystallized by layering pentane over its acetone solution. It exhibits a hydride signal at −21.71 ppm. The ^{19}F NMR spectrum of **9** exhibits a *broad* signal at −150 ppm, whereas free BF_4 gives a *sharp* signal at −151 ppm. Chemical shifts of coordinated BF_4 are reported in the range of −164 to −160 ppm, and the signal is usually broad because of fast rotation of bound BF_4.[24] In the case of **9**, the ^{19}F chemical shift and signal broadness indicate fast dissociative equilibrium of the anion in solution, with the equilibrium shifted toward free BF_4.

A single-crystal X-ray analysis of **9** (Figure 9, Table 6) confirmed the existence of a distorted octahedral structure with BF_4 coordinated through a fluorine atom (F(1)). F(1) is trans to the hydride ligand with an angle of 173.8°, whereas the chlorine atom is trans to the ipso nitrogen, with an angle of 177.68°. The B−F(1) bond (1.437 Å) is longer than the other B−F bonds (1.372−1.382 Å) as expected. The Rh−F(1) bond in **9** (2.407 Å) is longer than the reported Rh−F bonds in other coordinated BF_4 complexes[24a,b] by about 0.25 Å, which is consistent with the very weak nature of this bond.

Addition of acetonitrile to a solution of **9** in acetone afforded the complex [(PNP^{t}Bu)Rh(H)(Cl)(CH_3CN)][BF_4] (**10**) (Scheme 3), which exhibits a signal of free BF_4 in the ^{19}F NMR spectrum at −151 ppm and a triplet centered at −16.48 (J_{HP} = 12 Hz) ppm in the ^1H NMR spectrum.

A similar reaction was reported by Shaw and co-workers[30] for the Rh(II) complex $RhCl_2(P^tBuR_2)_2$ (R=Me, Et, ^{n}Pr), which, upon heating in ethanol or methyl ethyl ketone in the presence of excess of the phosphine ligand, gave Rh-(III) complex $RhCl_2H(P^tBuR_2)_2$. No explanation for this observation was given. The reduction of copper(II) chloride by triethylphosphine was reported to give the copper(I) complex $CuClPEt_3$. The oxidation product has not been characterized, although tertiary phosphine oxides have been obtained in similar wet systems.[31]

The reaction rate of **2** with triphenylphosphine is dependent on the amount of water in the solvent; in carefully dried acetone the reaction time is 12 h, whereas in wet acetone, obtained by the addition of a drop of water, the reaction reaches completion in a minute. Moreover, in methylene chloride, no reaction with triphenyphosphine takes place, but upon addition of water to this solution, **9** is obtained immediately. The formation of triphenyphosphine oxide and the influence of water concentration on the reaction rate indicate that Rh(II) complex **2** is reduced by Ph_3P and water

(29) (a) Goldberg, S. Z.; Kubiak, C.; Meyer, C. D.; Eisenberg, R. *Inorg. Chem.* **1975**, *14*, 1650−1654. (b) Hodgson, D. J.; Ibers, J. A. *Inorg. Chem.* **1968**, *7*, 2345−2352.

(30) (a) Masters, C.; Shaw, B. L. *J. Chem. Soc. A.* **1971**, 3679−3686. (b) Masters, C.; McDonald, W. S.; Raper, G.; Shaw, B. L. *Chem. Commun.* **1971**, 210−211.

(31) Axtell, D. D.; Yoke, J. T. *Inorg. Chem.* **1973**, *12*, 1265−1268 and references there in.

Scheme 4

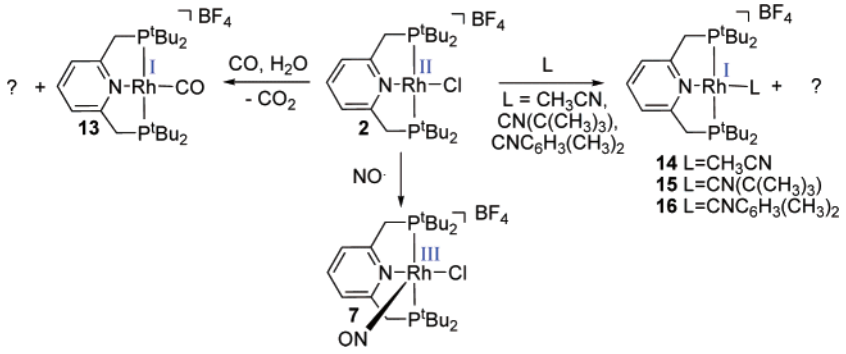

Scheme 5

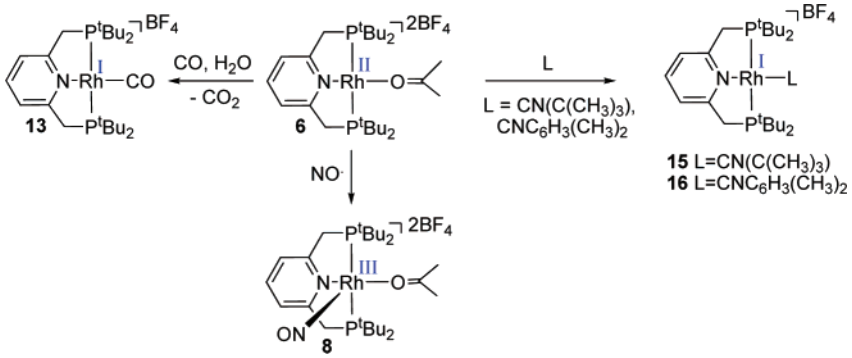

(eq 1). Neutral Rh(I) thus formed undergoes protonation to yield **9** (eq 2).

$$[(PNP)Rh^{II}(Cl)]^+ + 1/2Ph_3P + 1/2H_2O \rightarrow [(PNP)Rh^{I}Cl] + 1/2Ph_3PO + H^+ \quad (1)$$

$$[(PNP)Rh^{I}(Cl)] + H^+ \rightarrow [(PNP)Rh^{III}(H)(Cl)]^+ \quad (2)$$

Addition of the more-basic triethylposphine in excess to a wet acetone solution of Rh(II) complex **2** yielded a mixture of (PNP^{t}Bu)RhCl (**1**), [(PNP^{t}Bu)Rh(PEt$_3$)][BF$_4$] (**11**), and [PEt$_3$H][BF$_4$], according to ^{31}P NMR (Scheme 3).[32] The ^{31}P-{^{1}H} NMR spectrum of **11** exhibits a doublet of doublets at 67.87 ppm (J_{RhP} = 138.9, J_{PP} = 38.9 Hz) and a doublet of triplets at 25.33 ppm (J_{RhP} = 159.2, J_{PP} = 38.9 Hz) with an integration ratio of 2:1 respectively. **11** was also independently prepared by heating an acetone solution of cationic Rh(I) complex **5** with triethylphosphine at 55 °C for 1 h.

Dicationic Rh(II) complex **6** reacted slowly with 1.5 equiv of triphenylphosphine and an excess of water in acetone at ambient temperature to give Rh(I) complex [(PNP^{t}Bu)Rh-(PPh$_3$)][BF$_4$] (**12**) after 48 h (Scheme 3). The ^{31}P{^{1}H} NMR spectrum of **12** exhibits a doublet of doublets at 66.63 ppm (J_{RhP} = 134.8, J_{PP} = 38.1 Hz) and a doublet of triplets at 35.43 ppm (J_{RhP} = 171.3, J_{PP} = 38.1 Hz) with an integration ratio of 2:1 respectively. The ^{31}P{^{1}H} NMR spectrum of the reaction mixture also reveals a broad signal at 26 ppm, assignable to Ph$_3$PO, which disappears with time and a sharp signal at 44 ppm. **12** was also independently prepared like **11**.

In the case of dicationic Rh(II) complex **6**, reaction with triphenylphosphine and water leads to a less electron-rich cationic Rh(I) complex (eq 3), which does not undergo protonation. Having a vacant coordination site, it reacts with the excess triphenylphosphine to give **12** (eq 4).

$$[(PNP)Rh^{II}]^{2+} + 1/2Ph_3P + 1/2H_2O \rightarrow [(PNP)Rh^{I}]^+ + 1/2Ph_3PO + H^+ \quad (3)$$

$$[(PNP)Rh^{I}]^+ + PPh_3 \rightarrow [(PNP)Rh^{I}(PPh_3)]^+ \quad (4)$$

A similar reaction of Rh(II) complex **6** with excess triethylphosphine and water in acetone gave **11**.

Upon reaction of the Rh(II) complexes **2**, **4** and **6** with CO at ambient temperature, reduction to give cationic Rh(I) complex [(PNP^{t}Bu)Rh(CO)][X] (**13**) (X = Cl, BF$_4$, BAr^f, OC(O)CF$_3$) took place (Schemes 4, 5).[33] **13** was also prepared by reaction of CO with cationic Rh(I) complex **5**. The carbonyl ligand of this complex exhibits an IR band at 1982 cm^{-1}, and the carbonyl carbon has a chemical shift of

(32) (a) When less than one equiv of triethylphosphine was added to **2**, a mixture of [(PNP^{t}Bu)Rh(PEt$_3$)][BF$_4$] (**11**) and [(PNP^{t}Bu)Rh(Cl)(H)-(BF$_4$)] **(9)** was observed by ^{31}P{^{1}H} NMR. Addition of excess of triethylphosphine led to the deprotonation of **9** to **1**. (b) The ^{31}P{^{1}H} NMR spectrum of the reaction mixture reveals also singlets at 44.41 and 52.35 ppm, but no signal for the moisture-sensitive OPEt$_3$ was detected. [PEt$_3$H][OTf], formed by the addition of triflic acid to an acetone solution of triethylphosphine, gave a signal at 44.41 ppm.

(33) The presence of the non-coordinating BAr^f is significant in this reaction. Reaction of **4**, **6** and [(PNP^{t}Bu)RhCl][BArf] with CO gave exclusively **13**, whereas the reaction of [(PNP^{t}Bu)RhCl][BF$_4$] with CO afforded **13** as a major product (75% yield according to ^{31}P NMR) along with a new complex. Moreover, **4** and **6** react with one equiv of CO, whereas the reaction of **2** with CO required an excess for completion. The new complex exhibits, in the ^{31}P{^{1}H} NMR spectrum, a doublet at 54.4 ppm (J_{RhP} = 84.5 Hz) and in the ^{19}F NMR spectrum a broad signal at −149 ppm (coordinated BF$_4$). This complex is transformed to **13** with time under CO. We assume that the complex is [(PNP^{t}Bu)Rh(Cl)$_2$(BF$_4$)].

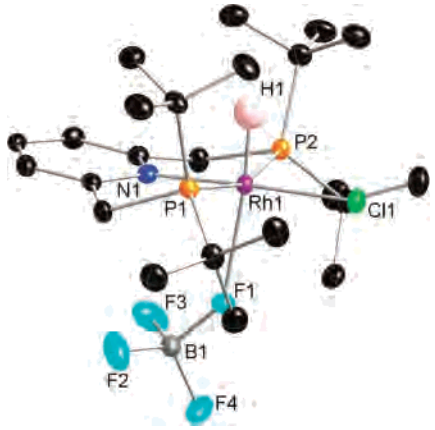

Figure 9. Molecular drawing of **9** at 50% probability level. Hydrogen atoms (except hydride) were omitted for clarity.

Table 6. Selected Bond Lengths (Angstroms) and Bond Angles (Degrees) for [(PNP^{t}Bu)Rh(Cl)(H)(BF$_4$)] (**9**)

Rh(1)−N(1)	2.045(2)	Rh(1)−F(1)	2.407(1)
Rh(1)−P(1)	2.327(1)	B(1)−F(1)	1.437(3)
Rh(1)−P(2)	2.324(1)	B(1)−F(2)	1.375(3)
Rh(1)−Cl(1)	2.345(1)	B(1)−F(3)	1.372(3)
Rh(1)−H(1)	1.43(3)	B(1)−F(4)	1.382(3)
H(1)−Rh(1)−P(1)	83.5(12)	P(2)−Rh(1)−Cl(1)	94.84(2)
H(1)−Rh(1)−P(2)	82.8(12)	P(2)−Rh(1)−F(1)	97.75(4)
H(1)−Rh(1)−F(1)	173.8(11)	N(1)−Rh(1)−F(1)	81.59(6)
H(1)−Rh(1)−Cl(1)	89.9(11)	N(1)−Rh(1)−Cl(1)	177.68(6)
P(1)−Rh(1)−Cl(1)	96.63(2)	N(1)−Rh(1)−P(1)	84.13(6)
P(1)−Rh(1)−P(2)	162.10(2)	N(1)−Rh(1)−P(2)	84.95(6)
P(1)−Rh(1)−F(1)	94.63(4)	N(1)−Rh(1)−H(1)	92.3(11)
Cl(1)−Rh(1)−F(1)	96.16(3)		

196.27 ppm (dt, J_{PC} = 13.4, J_{RhC} = 69.8 Hz) in the ^{13}C NMR spectrum. The X-ray structure of **13** (Figure 10) reveals a distorted square-planar geometry with a P−Rh−P angle of 168.05° and an N−Rh−C(24) angle of 175.19° (Figure 10).

GC-MS measurements of the gas phase indicated the formation of CO_2 in the reaction of **2** and **6** with CO. It is likely that a redox reaction involving CO and water, similar to the one with phosphines, is involved.

Reduction of Rh(II) to Rh(I) complexes in the presence of CO was observed with complexes [PBzPh$_3$]$_2$[Rh(C$_6$Cl$_5$)$_4$][19a] and with the two-legged piano-stool Rh(II) complex, which was reported by Mirkin and co-workers.[5a] In the latter case, the oxidation product was identified as CO_2. Disproportionation of a Rh(II) complex by CO was reported for the complex [Rh(tmpp)$_2$]$_2^+$ (tmpp = tris(2,4,6-trimethoxyphenyl)-phosphine).[28a]

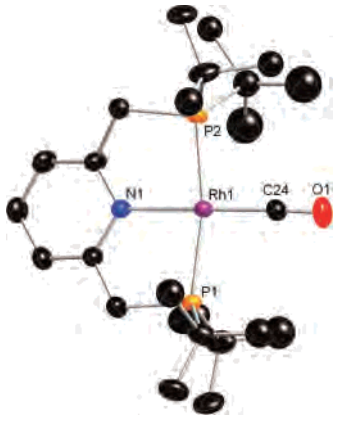

Figure 10. Molecular drawing of **13** at 30% probability level.[34] Hydrogen atoms and counteranion were omitted for clarity.

Table 7. Selected Bond Lengths (Anstroms) and Bond Angles (Degrees) for [(PNP^{t}Bu)Rh(CO)][BF$_4$] (**13**)

Rh(1)−P(1)	2.301(3)	Rh(1)−C(24)	1.818(5)
Rh(1)−P(2)	2.303(3)	Rh(1)−N(1)	2.100(4)
C(24)−O(1)	1.144(6)		
N(1)−Rh(1)−C(24)	175.19(18)	N(1)−Rh(1)−P(1)	84.05(10)
P(1)−Rh(1)−C(24)	95.66(15)	N(1)−Rh(1)−P(2)	84.00(10)
P(2)−Rh(1)−C(24)	96.24(15)	P(1)−Rh(1)−P(2)	168.05(4)
Rh(1)−C(24)−O(1)	177.5(5)		

Reaction of Rh(II) complex **2** with acetonitrile at room temperature led to formation of a diamagnetic mixture of two complexes in a ratio of 3:2, according to the ^{31}P{^{1}H} NMR spectrum (Scheme 4). The major complex was identified as the known [(PNP^{t}Bu)Rh(CH$_3$CN)][BF$_4$] (**14**).[8] The second complex exhibits in the ^{31}P{^{1}H} NMR spectrum a broad doublet at 60.2 ppm at 297 K, a sharp doublet at 61.36 ppm (J_{RhP} = 78.8) at 313 K, and an AB system at 55.24 and 63.54 ppm (J_{RhP} = 76.9 and J_{PP} = 479.8 Hz) at 230 K. The relatively small J_{RhP} coupling constant and the high field chemical shift of the minor complex suggest that it is a Rh(III) complex, although we were not able to determined its structure. To our knowledge, disproportionation of Rh(II) by acetonitrile was not reported. Reactions of Rh-(II) with isonitriles include the cleavage of methyl isonitrile by (TMP)Rh(II) (TMP = tetrakis(2,4,6-trimethylphenyl)-porphyrinato) to give (TMP)RhCN and (TMP)RhMe, reported by Wayland and co-workers.[35] Mirkin and co-workers reported the reduction of Rh(II) to Rh(I) by *tert*-butyl isonitrile.[5a] Wilkinson and co-workers reported the reduction of Rh(2,4,6,-^{i}Pr$_3$C$_6$H$_2$)(tht)$_2$ (tht = tetrahydrothiophene) by *tert*-butyl isonitrile to give Rh(CN^{t}Bu)$_3$(2,4,6,-^{i}Pr$_3$C$_6$H$_2$C=N^t-Bu).[36] This reduction was assumed to proceed via an aryl radical, which abstracts a hydrogen atom from the solvent. Disporprotonation of Rh(II) by methyl isonitrile was reported by Dunbar and Haefner, although the diamagnetic complexes were not identified.[37]

Reaction of **2** with one equiv of *tert*-butyl isonitrile in acetone also led to the formation of two diamagnetic complexes in a ratio of 17:3, according to the ^{31}P{^{1}H} NMR spectrum, of which the major product was identified as the Rh(I) complex [(PNP^{t}Bu)Rh(CNC(CH$_3$)$_3$)][BF$_4$] (**15**) (Scheme 4). **14** can be obtained also by the addition of *tert*-butyl isonitrile to **5**. The minor complex was not identified, although the chemical shift and the coupling constant (54.3 ppm (J_{RhP} = 84 Hz)) imply a Rh(III) complex. A similar reaction of **2** with 2,6-dimethylphenyl isonitrile also led to

(34) The X-ray diffraction of **13** was collected at 17° C because at lower temperature the crystals cracked.

(35) (a) Wayland, B. B.; Sherry, A. E.; Bunn, A. G. *J. Am. Chem. Soc.* **1993**, *115*, 7675−7684. (b) Poszmik, G.; Carroll, P. J.; Wayland, B. B. *Organometallics* **1993**, *12*, 3410−3417. For recent mechanistic studies see Zhang, L.; Fung, C. W.; Chan, K. S. *Organometallics* **2006**, *25*, 5381−89.

(36) Hay-Motherwell, R. S.; Koschmieder, S. U.; Wilkinson, G.; Hussain-Bates, B.; Hursthouse, M. B. *J. Chem. Soc., Dalton Trans.* **1991**, 2821−2830.

(37) Dunbar, K. R.; Haefner, S. C. *Organometallics* **1992**, *11*, 1431−1433.

the formation of two diamagnetic complexes, one of them being [(PNP^{t}Bu)Rh(CNC$_6$H$_3$(CH$_3$)$_2$)][BF$_4$] (**16**).

In contrast to monocationic Rh(II)Cl complex **2**, dicationic Rh(II)(acetone) complex **6** does not react with acetonitrile. It reacts with *tert*-butyl isonitrile and 2,6-dimethylphenyl isonitrile in acetone to give exclusively Rh(I) complexes **14** and **15,** respectively (Scheme 5).

Rh(II) chloride monocationic complex **2** and dicationic complex **6** exhibit different reactivity. Whereas **6** is reduced in the presence of triphenylphosphine, CO, and isonitriles, **2** undergoes disproportionation when reacted with CO, acetonitrile, and isonitriles. Reaction of **2** with triphenylphosphine leads to the protonation product **9**.[38] Also, as demonstrated by cyclic voltammetry, **6** exhibits a redox wave of Rh(II)/Rh(III), whereas **2** is irreversibly oxidized to Rh(III). Thus, the chloride ligand of **2** plays an important role in its redox reactivity. It seems that the chloride stabilizes the product Rh(III) complex, probably by π donation. The shortening of the Rh−Cl bond length as a result of the oxidation of Rh(I)Cl (**1**) to Rh(II)Cl (**2**), as evidenced from the X-ray structures of **1** and **2**, supports this assumption.

Conclusions

Paramagnetic monomeric (PNP^{t}Bu)Rh(II) complexes were prepared by the oxidation of (PNP^{t}Bu)Rh(I) complexes with AgX (X = BF$_4$, PF$_6$, BAr^f), whereas with AgOC(O)CF$_3$, chloride abstraction without oxidation to Rh(II) was observed. The Rh(II) complexes were characterized by X-ray diffraction, EPR, cyclic voltammetry, and dipole moment. The electron-rich, bulky tridentate PNP^{t}Bu ligand facilitates the oxidation of Rh(I) complexes on one hand, and on the other hand, the *tert*-butyl substituents stabilize the monomeric Rh(II) d^7 configuration by preventing dimerization. Although the paramagnetic complexes are relatively stable, they exhibit interesting reactivity. Mono- and dicationic Rh(II) complexes [(PNP^{t}Bu)RhCl][BF$_4$] (**2**) and [(PNP^{t}Bu)Rh(acetone)][BF$_4$]$_2$ (**6**) exhibit different reactivity patterns. Whereas **6** is reduced to Rh(I) in the presence of isonitriles or CO, **2** disproportionates in the presence of acetonitrile, isonitriles, or CO. **2** and **6** are reduced in the presence of phosphines and water to Rh(I) complexes. In the case of **2** and triphenylphosphine, the reduced Rh(I) complex undergoes protonation to give a Rh(III) complex with a coordinated BF$_4$ [(PNP^{t}Bu)Rh(Cl)(H)(BF$_4$)] (**9**).

Experimental Section

General Procedures. All of the experiments with metal complexes and phosphine ligands were carried out under an atmosphere of purified nitrogen in a Vacuum Atmospheres glove box equipped with a MO 40−2 inert gas purifier or using standard Schlenk techniques. All of the solvents were reagent grade or better. All of the non-deuterated solvents were refluxed over sodium/benzophenone ketyl and distilled under an argon atmosphere.

Deuterated solvents were used as received. All of the solvents were degassed with argon and kept in the glove box over 4 Å molecular sieves (acetone was kept over calcium sulfate). Commercially available reagents were used as received. ^{1}H, ^{13}C, ^{31}P, and ^{19}F NMR spectra were recorded using a Bruker DPX-250, a Bruker AMX-400, and an Avance 500 NMR spectrometer. All of the spectra were recorded at 23 °C, unless otherwise noted. ^{1}H NMR and ^{13}C{^{1}H} NMR chemical shifts are reported in ppm, downfield from tetramethylsilane. In ^{1}H NMR, chemical shifts were referenced to the residual hydrogen signal of the deuterated solvents. In ^{13}C{^{1}H} NMR measurements, the signals of deuterated solvents were used as a reference. ^{31}P NMR chemical shifts are reported in parts per million downfield from H_3PO_4 and referenced to an external 85% solution of phosphoric acid in D_2O. ^{19}F NMR chemical shifts were referenced to C_6F_6 (−163 ppm). Abbreviations used in the description of NMR data are as follows: br, broad; s, singlet; d, doublet; t, triplet; q, quartet; m, multiplet; v, virtual.

Cyclic voltammetric experiments were carried out using a CHI-660A potentiostat. A three-electrode setup was used for measurements consisting of a glassy-carbon working electrode, a platinum wire counter electrode, and an Ag/AgCl, KCl (sat'd) reference electrode. The measurements were performed using acetone solutions of the compounds (2×10^{-3} M) under nitrogen at room temperature (22 °C). ^{t}Bu$_4$NPF$_6$ (0.1 M) was used as a supporting electrolyte. Calibration was done with the ferrocenium/ferrocene couple (observed at 0.47 V).

Electron Paramagnetic Resonance (EPR) spectra were recorded on a ELEXSYS 500 spectrometer (Bruker, Germany) in 100 μL quartz capillary. The g values of the complexes in glassy solutions were determined using a 2,2-diphenyl-1-picrylhydrazyl (DPPH) resonance signal (g = 2.0037) as a standard. The variable temperature EPR experiments were carried out using a temperature unit (Euroterm, ER 4113VT, Bruker) with an accuracy of ±1 K.

Magnetic moments (dc and ac) of the powdered samples of **2** and **6** were measured using a Quantum Design Co. SQUID MPMS$_2$ field shielded magnetometer. The magnetic moment was measured versus field at T = 5 and 300 K at an increasing and decreasing field strength with ΔH = 0.01 T step inside of the interval −1 T ≤ H ≤ +1 T. Temperature dependencies of dc and ac magnetic susceptibility were taken at 0.5 T and with increasing the temperature from 2 to 300 K with 1 K steps using zero field cooled and field cooled modes. ac magnetic moment measurements were taken at a frequency of 700 Hz and a drive field amplitude 3 Oe.

[(PNP^{t}Bu)RhCl] (1). Crystals suitable for X-ray analysis were obtained by slow evaporation of the benzene solution of **1**.

X-ray Structural Analysis of 1. Crystal Data. $C_{23}H_{43}ClNP_2Rh$, red, 0.8 × 0.3 × 0.2 mm^3, hexagonal; *P*6/5 2 2 (No. 179); a = 16.275(2), b = 16.275(2), c = 19.222(4) Å; α = 90, β = 90, γ = 120°, from 20 degrees of data; T = 120(2) K; V = 4409.3(12) Å^3; Z = 6; fw = 533.88; D_c = 1.206 Mg/m^{-3}; μ = 0.789 mm^{-1}.

Data Collection and Processing. Nonius KappaCCD diffractometer, Mo Kα (λ = 0.71073 Å), graphite monochromator; 20 191 reflections collected, 0 ≤ h ≤ 21, −17 ≤ k ≤ 0, −24 ≤ l ≤ 24, frame scan width = 1.0°, scan speed 1.0° per 60 s, typical peak mosaicity 0.544°, 6717 independent reflections collected, (R_{int} = 0.034). The data were processed with Denzo-Scalepack.

Solution and Refinement. The structure was solved by direct methods with SHELXS-97. Full-matrix least-squares refinement based on F^2 with SHELXL-97; 136 parameters with 0 restraints, final R_1 = 0.0288 (based on F^2) for data with $I > 2\sigma(I)$, and R_1 = 0.0347 on 3357 reflections, GOF on F^2 = 1.006, largest electron density peak = 0.437 e Å^{-3}.

[(PNP^{t}Bu)RhCl][BF$_4$] (2). An acetone solution (5 mL) of AgBF$_4$ (21.8 mg, 0.112 mmol) was add to a red solution of (PNP^{t}Bu)RhCl (59.7 mg, 0.112 mmol) in 10 mL of acetone. The reaction mixture turned to green immediately, and a black precipitate was

(38) In the case of added PEt$_3$, the resulting deprotonation process masks the difference in redox reactivity between **2** and **6**.

formed. After stirring at ambient temperature for 30 min, the reaction mixture was filtered over celite, and the solvent was removed under a vacuum to give a green solid in quantitative yield. Crystals suitable for X-ray analysis were obtained by layering a concentrated acetone solution of **2** with pentane.

Anal. for $C_{23}H_{43}BClF_4NP_2Rh$, Calcd: C, 44.51; H, 6.98; Found: C, 44.62; H, 7.08.

X-ray Structural Analysis of 2. Crystal Data. $C_{23}H_{43}BClF_4NP_2Rh$, green, $1.1 \times 0.6 \times 0.4$ mm^3, monoclinic, $P2_1/c$ (No. 14); $a = 14.643(3)$, $b = 12.744(3)$, $c = 15.677(3)$ Å; $\beta = 105.67(3)°$ from 20 degrees of data; $T = 120(2)$ K; $V = 2815.0(10)$ Å^3; $Z = 4$; fw = 620.69; $D_c = 1.465$ Mg/m^{-3}; $\mu = 0.854$ mm^{-1}.

Data Collection and Processing. Nonius KappaCCD diffractometer, Mo Kα ($\lambda = 0.71073$ Å), graphite monochromator, 28 923 reflections collected, $-18 \le h \le 18$, $0 \le k \le 16$, $0 \le l \le 20$, frame scan width = 1.0°, scan speed 1.0° per 20 s, typical peak mosaicity 0.398°, 7430 independent reflections collected, ($R_{int} = 0.098$). The data were processed with Denzo-Scalepack.

Solution and Refinement. The structure was solved by direct methods with SHELXS-97. Full-matrix least-squares refinement based on F^2 and empirical absorption correction with SHELXL-97; 310 parameters with 0 restraints, final $R_1 = 0.0493$ (based on F^2) for data with $I > 2\sigma(I)$, and $R_1 = 0.0843$ on 6426 reflections, GOF on $F^2 = 1.006$, largest electron density peak = 1.640 e Å^{-3}.

[(PNP^{t}Bu)Rh(OC(O)CF$_3$)] (3). The same procedure as above was followed with (PNP^{t}Bu)RhCl (50 mg, 0.094 mmol) and AgOC(O)CF$_3$ (20.8 mg, 0.094 mmol) in acetone, to give a brown oil in quantitative yield.

^{31}P{^{1}H} NMR (101 MHz, THF-d_8): 61.27 (d, $J_{RhP} = 151.1$ Hz). ^{19}FNMR (235 MHz, THF-d_8): −76.59. ^{1}H NMR (400 MHz, THF-d_8): 1.38 (vt, 36H, $J_{PH} = 5.6$ Hz, C(*CH*$_3$)$_3$)), 3.13 (bs, 4H, *CH*$_2$-P), 7.01 (d, 2H, $^3J_{HH} = 6.8$ Hz, PNP-aryl H), 7.46 (t, 1H, $^3J_{HH} = 6.8$ Hz, PNP-aryl H). ^{13}C{^{1}H} NMR (101 Hz, THF-d_8): 29.52 (s, C(*CH*$_3$)$_3$)), 35.03 (vt, $J_{PC} = 6.0$ Hz, *C*(CH$_3$)$_3$)) 36.06 (vt, $J_{PC} = 6.0$ Hz, *CH*$_2$-P), 116.00 (q, $^1J_{CF} = 292.8$ Hz, C(O)*CF*$_3$) 120.67 (vt, $J_{PC} = 6.0$ Hz, 5.1 Hz, PNP aryl-CH), 130.48 (s, PNP aryl-CH), 161.31 (q, $^2J_{CF} = 33.2$ Hz, *C(O)*CF$_3$), 166.22 (vt, $J_{PC} = 6.0$ Hz, PNP aryl-C).

Anal. for $C_{25}H_{43}F_3NO_2P_2Rh$, Calcd: C, 49.11; H, 7.09; Found: C, 49.20; H, 6.95.

[(PNP^{t}Bu)Rh(OC(O)CF$_3$)][OC(O)CF$_3$] (4). The same procedure as above was followed with [(PNP^{t}Bu)Rh(OC(O)CF$_3$)] (30 mg, 0.049 mmol) and AgOC(O)CF$_3$ (10.8 mg, 0.049 mmol) in acetone to give a light-green solid in quantitative yield.

Anal. for $C_{27}H_{43}F_6NO_4P_2Rh$, Calcd: C, 44.76; H, 5.98; Found: C, 44.67; H, 6.08.

[(PNP^{t}Bu)Rh(acetone)][BF$_4$](5). An ether solution (5 mL) of PNP^{t}Bu (134.0 mg, 0.339 mmol) was added dropwise to an acetone solution (10 mL) of [Rh(COE)$_2$ (acetone)$_2$][BF$_4$] (178.2 mg, 0.339 mmol). Upon the addition of the PNP^{t}Bu ligand, the solution color turned from yellow to red. The reaction mixture was stirred for 5 min at ambient temperature, and then the solvent volume was reduced using a vacuum to 2 mL. The solution was poured into pentane, resulting in the precipitation of **5** as a red solid. The solid was separated by decantation and dried under a vacuum (207 mg, 95% yield). **5** is poorly soluble in benzene and reacts with chlorinated solvents.

^{31}P{^{1}H} NMR (162 MHz, acetone-d_6): 64.20 (d, $J_{RhP} = 144.0$ Hz). ^{1}H NMR (400 MHz, acetone-d_6): 1.34 (vt, 36H, $J_{PH} = 6.6$ Hz, C(*CH*$_3$)$_3$)), 3.44 (vt, $J_{PH} = 3.4$ Hz, 4H, *CH*$_2$-P), 7.27 (d, 2H, $^3J_{HH} = 7.3$ Hz, PNP-aryl H), 7.62 (t, 1H, $^3J_{HH} = 7.3$ Hz, PNP-aryl H). ^{13}C{^{1}H} NMR (100 Hz, acetone-d_6): 29.20 (s, C(*CH*$_3$)$_3$)), 34.77 (vt, $J_{PC} = 7.0$ Hz, *CH*$_2$-P), 35.00 (vt, $J_{PC} = 7.6$ Hz, *C*(CH$_3$)$_3$)), 121.22 (bs, PNP aryl-CH), 135.14 (s, PNP aryl-CH), 166.35 (vt, J_{PC}=5.4 Hz, PNP aryl-C).

Acceptable elemental analysis results for **5** could not be obtained due to the weakly coordinated acetone ligand.

[(PNP^{t}Bu)Rh(acetone)][BF$_4$]$_2$ (6). The same procedure as for **2** was followed with [(PNP^{t}Bu)Rh(acetone)][BF$_4$](60 mg, 0.093 mmol) and AgBF$_4$ (18.1 mg, 0.093 mmol), to give a brown oil in quantitative yield. Crystals suitable for X-ray analysis were obtained by layering a concentrated acetone solution of **6** with pentane.

Anal. for $C_{26}H_{49}B_2F_8NOP_2Rh$, Calcd: C, 42.77; H, 6.76; Found: C, 42.63; H, 6.75.

X-ray Structural Analysis of 6. Crystal Data. $C_{26}H_{49}B_2F_8NOP_2Rh$, orange, $1.0 \times 0.6 \times 0.3$ mm^3, monoclinic, $C2/c$; $a = 29.248(6)$, $b = 14.051(3)$, $c = 19.768(4)$ Å; $\beta = 125.59(3)°$, from 20 degrees of data; $T = 120(2)$ K; $V = 6670(2)$ Å^3; $Z = 8$; fw = 730.13; $D_c = 1.468$ Mg/m^{-3}; $\mu = 0.680$ mm^{-1}.

Data Collection and Processing. Nonius KappaCCD diffractometer, Mo Kα ($\lambda = 0.71073$ Å), graphite monochromator, 34 868 reflections collected, $-39 \le h \le 31$, $0 \le k \le 18$, $0 \le l \le 26$, frame scan width = 2.0°, scan speed 1.0° per 40 s, typical peak mosaicity 0.713°, 8683 independent reflections collected, ($R_{int} = 0.068$). The data were processed with Denzo-Scalepack.

Solution and Refinement. The structure was solved by direct methods with SHELXS-97. Full-matrix least-squares refinement based on F^2 and empirical absorption correction with SHELXL-97; 399 parameters with 0 restraints, final $R_1 = 0.0401$ (based on F^2) for data with $I > 2\sigma(I)$, and $R_1 = 0.0462$ on 8332 reflections, GOF on $F^2 = 0.986$, largest electron density peak = 1.531 e Å^{-3}.

[(PNP^{t}Bu)Rh (NO)Cl][BF$_4$] (7). A green solution of [(PNP^t-Bu)RhCl][BF$_4$](**2**) (20 mg, 0.032 mmol) in acetone (2 mL) was exposed to 1 atm of NO at ambient temperature. The solution turned to light-green. The solvent was removed under a vacuum to give a green solid as **7** in quantitative yield. Crystals suitable for X-ray analysis were obtained by layering a concentrated acetone solution of **7** with pentane.

7 was obtained also by the addition of NOBF$_4$ (3.0 mg, 0.027 mmol) in acetone (5 mL) to a solution of (PNP^{t}Bu)RhCl (14.5 mg, 0.027 mmol) in acetone (5 mL). ^{31}P{^{1}H} NMR (101 MHz, acetone-d_6): 67.2 (d, $J_{RhP} = 114$ Hz). ^{1}HNMR (500 MHz, acetone-d_6): 1.33 (vt, 18H, $J_{PH} = 7.5$ Hz, C(*CH*$_3$)$_3$)), 1.43 (vt, 18H, $J_{PH} = 7.3$ Hz, C(*CH*$_3$)$_3$)), 4.13(d of vt, 2H, $J_{PH} = 3.7$ Hz, $^2J_{HH} = 18.4$ Hz, *CH*$_2$-P), 4.30 (d of vt, 2H, $J_{PH} = 5.5$ Hz, $^2J_{HH} = 18.4$ Hz, *CH*$_2$-P), 7.89 (d, 2H, $^3J_{HH} = 7.6$ Hz, PNP-aryl H), 8.13 (t, 1H, $^3J_{HH} = 7.6$ Hz, PNP-aryl H). ^{13}C{^{1}H} NMR (126 Hz, acetone-d_6): 28.20 (s, C(*CH*$_3$)$_3$)), 34.43 (vt, $J_{PC} = 9.5$ Hz, *CH*$_2$-P), 36.82 (vt, $J_{PC} = 8.1$ Hz, *C*(CH$_3$)$_3$)), 38.37 (vt, $J_{PC} = 8.0$ Hz, *C*(CH$_3$)$_3$)), 124.02 (vt, $J_{PC} = 5.3$ Hz, PNP aryl-CH), 141.20 (s, PNP aryl-CH), 165.69 (vt, $J_{PC} = 2.9$ Hz, PNP aryl-C). IR (ν_{NO}) = 1675 cm^{-1}.

Anal. for $C_{23}H_{43}BClF_4N_2OP_2Rh$, Calcd: C, 42.45; H, 6.66; Found: C, 42.55; H, 6.75.

X-ray Structural Analysis of 7. Crystal Data. $C_{23}H_{43}BClF_4N_2OP_2Rh$, orange, $0.8 \times 0.6 \times 0.2$ mm^3, monoclinic, $P2_1/n$; $a = 12.526(3)$, $b = 7.8930(16)$, $c = 28.603(6)$ Å; $\beta = 93.36(3)°$, from 20 degrees of data; T =120(2) K; $V = 2823.0(10)$ Å^3; $Z = 4$; fw = 650.70; $D_c = 1.531$ Mg/m^{-3}; $\mu = 0.859$ mm^{-1}.

Data Collection and Processing. Nonius KappaCCD diffractometer, Mo Kα ($\lambda = 0.71073$ Å), graphite monochromator, 18 807 reflections collected, $-16 \le h \le 16$, $0 \le k \le 10$, $0 \le l \le 37$, frame scan width = 2.0°, scan speed 1.0° per 20 s, typical peak mosaicity 0.496°, 6842 independent reflections collected, ($R_{int} = 0.042$). The data were processed with Denzo-Scalepack.

Solution and Refinement. The structure was solved by direct methods with SHELXS-97. Full-matrix least-squares refinement

based on F^2 and empirical absorption correction with SHELXL-97; 328 parameters with 0 restraints, final $R_1 = 0.0401$ (based on F^2) for data with $I > 2\sigma(I)$, and $R_1 = 0.0571$ on 6379 reflections, GOF on $F^2 = 1.017$, largest electron density peak = 1.692 e Å^{-3}.

[(PNP^{t}Bu)Rh(acetone)(NO)][BF$_4$]$_2$ (8). The same procedure as above was followed with [(PNP^{t}Bu)Rh(acetone)][BF$_4$]$_2$ (**6**).

^{31}P{^{1}H} NMR (101 MHz, acetone-d_6): 67.73 (d, $J_{RhP} = 122$ Hz). ^{1}H NMR (400 MHz, acetone-d_6): 1.17(vt, 18H, $J_{PH} = 7.6$ Hz, C(CH_3)$_3$)), 1.38 (vt, 18H, $J_{PH} = 7.6$ Hz, C(CH_3)$_3$)), 4.11(d of vt, 2H, $J_{PH} = 4.4$ Hz, $^2J_{HH} = 18.6$ Hz, CH_2-P), 4.30 (d of vt, 2H, $J_{PH} = 4.4$ Hz, $^2J_{HH} = 18.6$ Hz, CH_2-P), 7.89 (d, 2H, $^3J_{HH} = 7.7$ Hz, PNP-aryl H), 8.17 (t, 1H, $^3J_{HH} = 7.7$ Hz, PNP-aryl H). ^{13}C-{^{1}H} NMR (101 Hz, acetone-d_6): 29.40 (s, C(CH_3)$_3$)), 34.26 (vt, $J_{PC} = 10.0$ Hz, CH_2-P), 39.11(vt, $J_{PC} = 8.2$ Hz, C(CH$_3$)$_3$)), 124.44 (vt, $J_{PC} = 6.1$ Hz, PNP aryl-CH), 142.17 (s, PNP aryl-CH), 165.10 (vt, $J_{PC} = 3.0$ Hz, PNP aryl-C). IR (ν_{NO}) = 1706 cm^{-1}.

Anal. for $C_{26}H_{49}B_2F_8IrN_2O_2P_2Rh$, Calcd: C, 41.08; H, 6.50; Found: C, 41.17; H, 6.58.

[(PNP^{t}Bu)Rh(Cl)(H)(BF$_4$)] (9). To an acetone solution (2 mL) of **2** (20 mg, 0.032 mmol) was added PPh_3 (8.4 mg, 0.032 mmol) in acetone (2 mL). A drop of water was added to the reaction mixture, and the color changed immediately from green to orange. The solvent was removed under a vacuum, and the residue was redissolved in 1 mL of acetone. ^{31}P NMR indicated the disappearance of the paramagnetic complex and the formation of **9** as the only metal complex. Crystals of **9** were obtained by layering pentane over the acetone solution. The crystals were washed with pentane and redissolved in acetone for NMR analysis. Crystals for X-ray analysis were produced in the same way.

^{31}P{^{1}H} NMR (101 MHz, acetone-d_6): 67.23 (d, $J_{RhP} = 99.9$ Hz) ^{1}H NMR (500 MHz, acetone-d6): −21.71 (m, 1H, Rh−H), 1.33(vt, 18H, $J_{PH} = 6.8$ Hz, C(CH$_3$)$_3$)), 1.36 (vt, 18H, $J_{PH} = 6.7$ Hz, C(CH$_3$)$_3$)), 3.87 (bd, 2H, $^2J_{HH} = 17.6$ Hz, CH_2-P), 3.97 (bd, 2H, $^2J_{HH} = 17.6$ Hz, CH_2-P), 7.59 (d, 2H, $^3J_{HH} = 7.4$ Hz, PNP-aryl H), 8.86 (t, 1H, $^3J_{HH} = 7.4$ Hz, PNP-aryl H). ^{13}C{^{1}H} NMR-(125 Hz, acetone-d_6): 29.03 (s, C(CH_3)$_3$)) 29.14 (s, C(CH_3)$_3$)), 35.77 (vt, $J_{PC} = 8.2$ Hz, CH_2-P), 36.28 (vt, $J_{PC} = 9.4$ Hz, C(CH$_3$)$_3$)), 36.90 (vt, $J_{PC} = 7.5$ Hz, C(CH$_3$)$_3$)), 122.78 (vt, $J_{PC} = 4.4$ Hz, PNP aryl-CH), 140.09 (s, PNP aryl-CH), 166.02 (vt, $J_{PC} = 3.1$ Hz PNP aryl-C).

X-ray Structural Analysis of 9. Crystal Data. $C_{23}H_{44}BClF_4NP_2Rh$, orange, 0.4 × 0.3 × 0.2 mm^3, monoclinic, $P2_1/c$ (No. 2); $a = 18.5010(3)$, $b = 10.9900(4)$, $c = 15.2180(7)$ Å; $\beta = 111.949(2)°$, from 20 degrees of data; T =120(2) K; $V = 2869.9(2)$ Å^3; $Z = 4$; fw = 621.70; $D_c = 1.439$ Mg/m^{-3}; $\mu = 0.838$ mm^{-1}.

Data Collection and Processing. Nonius KappaCCD diffractometer, Mo Kα ($\lambda = 0.71073$ Å), graphite monochromator, 25 884 reflections collected, $-24 \le h \le 22$, $0 \le k \le 14$, $0 \le l \le 19$, frame scan width = 2.0°, scan speed 1.0° per 20 s, typical peak mosaicity 0.59°, 6895 independent reflections collected, ($R_{int} = 0.053$). The data were processed with Denzo-Scalepack.

Solution and Refinement. The structure was solved by direct methods with SHELXS-97. Full-matrix least-squares refinement based on F^2 and empirical absorption correction with SHELXL-97; 302 parameters with 0 restraints, final $R_1 = 0.0345$ (based on F^2) for data with $I > 2\sigma(I)$, and $R_1 = 0.0561$ on 6554 reflections, GOF on $F^2 = 1.015$, largest electron density peak = 1.081 e Å^{-3}.

[(PNP^{t}Bu)Rh(Cl)(H)(CH$_3$CN)][BF$_4$] (10). To a solution of **9** in acetone (15 mg, 0.024 mmol) in a NMR tube was added acetonitrile (1.26μL, 0.024 mmol). The color changed from orange to yellow.

^{31}P{^{1}H} NMR (101 MHz, acetone-d_6): 68.61 (d, $J_{RhP} = 99.3$ Hz) ^{1}H NMR (500 MHz, acetone-d6): −16.48 (bd, 1H, $J_{RhP} = 12$ Hz, Rh−H), 1.37 (vt, 36H, $J_{PH} = 7.3$ Hz, C(CH$_3$)$_3$)), 3.61 (bd, 2H, $^2J_{HH} = 16.5$ Hz, CH$_2$−P), 3.94 (bd, 2H, $^2J_{HH} = 16.5$ Hz, CH$_2$−P), 7.59 (d, 2H, $^3J_{HH} = 7.4$ Hz, PNP-aryl H), 8.86 (t, 1H, $^3J_{HH} = 7.4$ Hz, PNP-aryl H). ^{13}C{^{1}H} NMR (125 Hz, acetone-d_6): 1.95 (s, CH_3CN), 29.29 (vt, $J_{PC} = 3.3$ Hz C(CH_3)$_3$)), 36.53 (vt, $J_{PC} = 8.2$ Hz, CH_2-P) 37.69 (vt, $J_{PC} = 7.2$ Hz, C(CH$_3$)$_3$)), 121.46 (vt, $J_{PC} = 5.9$ Hz, PNP aryl-CH), 139.42 (s, PNP aryl-CH), 165.56 (vt, $J_{PC} = 3.6$ Hz PNP aryl-C). A signal for CH_3CN was not detected.

[(PNP^{t}Bu)Rh(PEt$_3$)][BF$_4$] (11). To an acetone solution (2 mL) of **6** (20 mg, 0.027 mmol) a large excess of PEt_3 and a drop of water were added. The reaction mixture was stirred for 30 min at ambient temperature, during which the color changed from brown to light red. The solvent was removed under a vacuum to give **11** as an orange solid in quantitative yield. **11** can also be obtained by heating a solution of **5** in acetone with PEt_3 for 1 h at 50 °C.

^{31}P{^{1}H} NMR (101 MHz, acetone-d_6): 25.33 (1P, dt, $J_{RhP} = 159.2$ Hz, $J_{PP} = 38.9$ Hz), 67.87 (2P, dd, $J_{Rhp} = 138.9$ Hz, $J_{PP} = 38.9$ Hz). ^{1}H NMR (400 MHz, acetone-d6): 1.21 (m, 9H, P(CH$_2$$CH_3$)$_3$), 1.34 (vt, 36H, $J_{PH} = 4.0$ Hz, C(CH$_3$)$_3$)), 2.03 (quin., 6H, $J = 7.5$ Hz, P(CH_2CH$_3$)$_3$), 3.78 (bs, 4H, CH$_2$−P), 7.61 (d, 2H, $^3J_{HH} = 7.5$ Hz, PNP-aryl H), 7.90 (t, 1H, $^3J_{HH} = 7.5$ Hz, PNP-aryl H). ^{13}C{^{1}H} NMR (125 Hz, acetone-d_6): 9.38 (bs, P(CH$_2$$CH_3$)$_3$), 24.38 (b dd, $J = 2.1$, 26.7 Hz, P(CH_2CH$_3$)$_3$), 30.89 (vt, $J_{PC} = 3.0$ Hz C(CH_3)$_3$)), 36.60 (dvt, $J = 2.6$, 5.9 Hz, C(CH$_3$)$_3$)) 38.51 (dvt, $J = 1.9$, 8.15 Hz, CH_2-P), 121.37 (bs, PNP aryl-CH), 139.52 (s, PNP aryl-CH), 162.33 (vt, $J_{PC} = 7.5$ Hz PNP aryl-C).

Anal. for $C_{29}H_{58}BF_4NP_3Rh$, Calcd: C, 49.52; H, 8.31; Found: C, 49.36; H, 8.40.

[(PNP^{t}Bu)Rh(PPh$_3$)][BF$_4$] (12). To an acetone solution (2 mL) of **6** (20 mg, 0.027 mmol) PPh_3 (10.5 mg, 0.040 mmol) in acetone (2 mL) and a drop of water were added. The reaction mixture was stirred for 2 days at ambient temperature, during which the color changed from brown to light yellow and finally to orange. The solvent was removed under a vacuum to give **11** as a red oil in quantitative yield. **11** can also be obtained by heating a solution of **5** in acetone with an equivalent amount of triphenylphosphine for 4 h at 50 °C.

^{31}P{^{1}H} NMR (101 MHz, acetone-d_6): 35.43 (dt, 1P, $J_{RhP} = 171.3$ Hz, $J_{PP} = 38.1$ Hz), 66.63 (dd, 2P, $J_{RhP} = 134.8$ Hz, $J_{PP} = 38.1$ Hz). ^{1}H NMR (400 MHz, acetone-d6): 0.9 (vt, 36H, J_{PH}=6.6 Hz, C(CH_3)$_3$)), 3.77 (bt, 4H, J_{PH}=3.9 Hz, CH$_2$−P),7.4 (bs, 9H, RhPPh$_3$), 7.66 (d, 2H, $^3J_{HH}$ =7.9 Hz, PNP-aryl H), 7.95 (t, 1H, $^3J_{HH}$=7.9 Hz, PNP-aryl H), 8.12−8.08 (m, 6H, RhPPh$_3$). ^{13}C{^{1}H} NMR (125 Hz, acetone-d_6): 30.07 (s, C(CH_3)$_3$)) 30.09 (s, C(CH_3)$_3$)), 36.57 (vt, $J_{PC} = 6.5$ Hz, C(CH$_3$)$_3$)) 38.05 (vt, $J_{PC} = 7.0$ Hz, CH_2-P), 121.48 (s, PNP aryl-CH), 128.70 (d, $J_{PC} = 9.0$ Hz, RhPPh$_3$), 131.16 (d, $J_{PC} = 2.0$ Hz, RhPPh$_3$), 136.57 (d, $J_{PC} = 12.1$ Hz, RhPPh$_3$), 139.68 (s, PNP aryl-CH), 141.01 (d, $J_{PC} = 39.2$ Hz, RhPPh$_3$), 162.67 (bs, PNP aryl-C).

Anal. for $C_{41}H_{58}BF_4NP_3Rh$, Calcd: C, 58.10; H, 6.90; Found: C, 57.94; H, 6.82.

[(PNP^{t}Bu)Rh(CO)][X] (X = BF$_4$, BAr^f, OC(O)CF$_3$, Cl) (13). To an acetone solution (0.5 mL) of **2**, **5** and **6** (20 mg, 0.032, 0.031 and 0.027 mmol respectively) in a septum-capped NMR tube was bubbled CO. The color changed to yellow, and **13** was immediately formed. The solvent was removed under a vacuum, resulting in a yellow solid in quantitative yield. Crystals suitable for X-ray analysis were obtained by layering a concentrated acetone solution of **13** with pentane.

^{31}P{^{1}H} NMR (101 MHz, acetone-d_6): 79.84 (d, $J_{RhP} = 120.0$ Hz). ^{1}H NMR (400 MHz, acetone-d_6): 1.40 (vt, 36H, $J_{PH} = 7.3$ Hz, C(CH_3)$_3$)), 4.11 (vt, 4H, $J_{PH} = 3.8$ Hz, CH_2-P), 7.70 (d, 2H, $^3J_{HH} = 7.6$ Hz, PNP-aryl H), 7.97 (t, 1H, $^3J_{HH} = 7.6$ Hz, PNP-aryl

H). $^{13}C\{^1H\}$ NMR (101 Hz, acetone-d_6): 29.42 (s, C(CH_3)$_3$)), 43.29 (vt, J_{PC} = 6.5 Hz, CH_2-P), 43.29 (vt, J_{PC} = 6.5 Hz, C(CH$_3$)$_3$)), 122.69 (vt, J_{PC} = 4.5 Hz, PNP aryl-CH), 141.57 (s, PNP aryl-CH), 166.43 (vt, J_{PC} = 7.5 Hz, PNP aryl-C) 196.27 (dt, J_{PC} = 13.4 Hz, J_{RhC} = 69.8 Hz, Rh*C*O). IR (ν_{CO}) = 1982 cm^{-1}

Anal. for $C_{24}H_{43}BF_4NOP_2Rh$, Calcd: C, 47.00; H, 7.07; Found: C, 48.08; H, 7.18.

X-ray Structural Analysis of 13. Crystal Data. $C_{24}H_{43}BF_4NOP_2Rh$, yellow, 0.1 × 0.1 × 0.05 mm^3, triclinic, $P\bar{1}$; a = 8.0990(2), b = 12.3870(2), c = 15.5640(3) Å; α =107.840(1), β = 102.825(1), γ = 91.456(1)°, from 20 degrees of data; T = 290(2) K; V = 1441.90(5) Å^3; Z = 2; fw = 613.26; D_c = 1.412 Mg/m^{-3}; μ = 0.746 mm^{-1}.

Data Collection and Processing. Nonius KappaCCD diffractometer, Mo Kα (λ = 0.71073 Å), graphite monochromator, 16 163 reflections collected, $-10 \le h \le 10$, $-16 \le k \le 15$, $0 \le l \le 20$, frame scan width = 1.0°, scan speed 1.0° per 60 s, typical peak mosaicity 0.842°, 6282 independent reflections collected, (R_{int} = 0.040). The data were processed with Denzo-Scalepack.

Solution and Refinement. The structure was solved by the Patterson method with SHELXS-97. Full-matrix least-squares refinement based on F^2 and empirical absorption correction with SHELXL-97; 284 parameters with 2 restraints, final R_1 = 0.0582 (based on F^2) for data with $I > 2\sigma(I)$, and R_1 = 0.0653 on 6273 reflections, GOF on F^2 = 1.069, largest electron density peak = 1.090 e Å^{-3}.

[(PNP^{t}Bu)Rh(CNC(CH$_3$)$_3$)][BF$_4$] (15). To an acetone solution of **2**, **5** and **6** (20 mg, 0.032, 0.031 and 0.027 mmol respectively) one equiv of *tert*-butyl isocyanide was added, and the color changed to orange. The solvent was removed under a vacuum, resulting in a yellow solid in quantitative yield (in case of **5** and **6**).

$^{31}P\{^1H\}$ NMR (101 MHz, acetone-d_6): 73.91 (d, J_{RhP} = 131.1 Hz). ^1H NMR (400 MHz, acetone-d_6): 1.45 (bs, 36, C(CH_3)$_3$)), 1.52 (s, 9H, CNC(CH_3)$_3$)), 3.85 (vt, 4H, J_{PH} = 3.7 Hz, CH_2-P), 7.58 (d, 2H, $^3J_{HH}$ = 7.8 Hz, PNP-aryl H), 7.86 (t, 1H, $^3J_{HH}$ = 7.8 Hz, PNP-aryl H). $^{13}C\{^1H\}$ NMR (101 Hz, acetone-d_6): 29.43 (vt, J_{PC} = 3.4 Hz C(CH_3)$_3$)), 30.57 (s, NC(CH_3)$_3$), 35.87 (vt, J_{PC} = 8.5 Hz, C(CH$_3$)$_3$)), 36.61(vt, J_{PC} = 8.0 Hz, CH_2-P), 58 (s, NC(CH$_3$)$_3$), 121.73 (vt, J_{PC} = 6.5 Hz, PNP aryl-CH), 139.10 (s, PNP aryl-CH), 145.8 (bd, J_{RhC} = 75 Hz, Rh*C*), 165.87 (vt, J_{PC} = 5.0 Hz, PNP aryl-C). IR ($\nu_{C\equiv N}$) = 2104 cm^{-1}.

Anal. for $C_{28}H_{52}BF_4N_2P_2Rh$, Calcd: C, 50.32; H, 7.84; Found: C, 49.86; H, 7.67.

[(PNP^{t}Bu)Rh(CNC$_6$H$_3$(CH$_3$)$_2$)][BF$_4$] (16). The same procedure as above was followed with **2**, **5** and **6**, and 2,6-dimethylphenyl isonitrile.

$^{31}P\{^1H\}$ NMR (161 MHz, acetone-d_6): 78.05 (d, J_{RhP} = 128.2 Hz). ^1H NMR (400 MHz, acetone-d_6): 1.40 (vt, 36H, J_{PH} = 7.3 Hz C(CH_3)$_3$)), 2.42 (s, 6H, CN(C$_6$H$_3$(CH_3)$_2$)), 3.94 (vt, 4H, J_{PH} = 4.0 Hz, CH_2-P), 7.17 (bs, 3H, CN(C$_6$H$_3$(CH$_3$)$_2$)), 7.62 (d, 2H, $^3J_{HH}$ = 7.3 Hz, PNP-aryl H), 7.90 (t, 1H, $^3J_{HH}$ = 7.3 Hz, PNP-aryl H). $^{13}C\{^1H\}$ NMR (101 Hz, acetone-d_6): 18.88 (s, CN(C$_6$H$_3$(CH_3)$_2$)), 29.40 (vt, J_{PC} = 3.0 Hz C(CH_3)$_3$)), 36.08 (vt, J_{PC} = 8.5 Hz, C(CH$_3$)$_3$)), 36.40 (vt, J_{PC} = 8.4 Hz, CH_2-P), 122.01 (vt, J_{PC} = 5.1 Hz, PNP aryl-CH),128.34 (s, C4 - NC(C$_6$$H_3(Me)_2$)), 128.98 (s, C3, C5 - CN(C$_6$$H_3$(CH$_3$)$_2$)), 129.57 (s, C1 - CN(C$_6$$H_3$(CH$_3$)$_2$)), 134.02 (s, *C*2, C6 - CN(C$_6$$H_3$(CH$_3$)$_2$)), 139.80 (s, PNP aryl-CH), 165.96 (vt, J_{PC} = 6.0 Hz, PNP aryl-C). IR ($\nu_{C\equiv N}$) = 2077 cm^{-1}.

Anal. for $C_{33}H_{56}BF_4N_2P_2Rh$, Calcd: C, 54.11; H, 7.71; Found: C, 53.88; H, 7.66.

Acknowledgment. This work was supported by the Israel Science Foundation, by the DIP program for German-Israeli cooperation, by the MINERVA foundation, and by The Helen and Martin Kimmel Center for Molecular Design. D.M. holds the Israel Matz Professorial Chair of Organic Chemistry.

Supporting Information Available: CIF files containing X-ray crystallographic data for **1**, **2**, **6**, **7**, **9**, and **13**. Correlation of peak current versus scan rate for first reversible redox process of **1**, **2**, **5** and **6**. This material is available free of charge via the Internet at http://pubs.acs.org.

IC701044B